J. Fluid Mech. (1977), *vol.* 79, *part* 4, *pp.* 631–655
Printed in Great Britain

Upstream interactions in channel flows

By F. T. SMITH

Department of Mathematics, Imperial College, London

(Received 24 July 1975 and in revised form 19 January 1976)

The manner in which fluid driven through a channel of width a responds in anticipation of a severe asymmetric distortion (e.g. to the wall or interior conditions downstream) is discussed when the oncoming flow is fully developed, the characteristic Reynolds number K is large and the whole motion remains laminar. Far ahead of the disturbance, at distances $O(aK^{\frac{1}{7}})$, there occurs a free interaction which triggers a small displacement in the core, generating viscous layers near both walls; the relatively large induced pressure gradient acting *across* the channel is then found to sustain the growth of this displacement. Numerical solutions of the fundamental nonlinear problem show that one layer separates in a regular fashion, but that beyond separation the other layer, under compression, produces a singularity in the interaction. Analysis of the singularity based on a self-similar structure in the partly reversed flow then leads to a description of the nonlinear flow features nearer the distortion which seems to have strong physical significance. The major implication is that the flow will have already separated at one wall, and developed a definite nonlinear character quite distinct from that of the original Poiseuille flow, long before it reaches finite distances from the distortion. The separation point is predicted to be a distance $0{\cdot}49aK^{\frac{1}{7}}$ $(+O(a))$ ahead of the particular finite distortion. Comparisons of this and other predictions with computed solutions of the full Navier–Stokes equations show reasonable agreement.

1. Introduction

The principal question around which the present work is centred concerns the effects on the otherwise undirectional flow field within a long straight rigid-walled channel of a severe asymmetric disturbance at some downstream station. If, for example, a constriction is introduced at the channel wall or in the interior, if the channel branches, or if extra fluid is injected from the wall, how does the laminar flow of the incompressable fluid in the channel ahead of the disturbance anticipate the presence of this alteration in the boundary conditions? We shall assume that the flow sufficiently far upstream is fully developed, that it remains steady and two-dimensional throughout and that the characteristic Reynolds number K is large. Our especial interest then is in the most realistic cases, where the particular disturbance is large enough to provoke a *finite* change in the flow pattern. Thus we should like to gain some knowledge of the upstream response of the fluid when the shape of the channel is changed appreciably, by an abrupt

halving of its width, for instance, or when the injection rate is comparable with the velocity of the oncoming Poiseuille motion.

In the corresponding exterior flow situations where one of the plane walls is absent and the inviscid mainstream is uniform, say, a severe wall disturbance, no matter how far from the leading edge, could well provoke separation of the boundary layer upstream. The free interaction here by which the boundary layer evolves from the Blasius profile to a separated profile in supersonic flow is described by the triple-deck theory of Stewartson (1974). The displacement thickness starts to increase, promoting a decrease in the pressure just outside the boundary layer which in turn reinforces the thickening process, and so the boundary layer moves towards a separated structure (Stewartson & Williams 1969, 1973). Treatments of injection, cornering and indentation problems on those lines have been given by Smith & Stewartson (1973), Stewartson (1970) and Smith (1973).

In channels and pipes, on the other hand, if we move the disturbance further and further from the inlet the walls tend to suppress this type of upstream influence, as Smith (1976*c*) shows, and ultimately such a mainstream interaction becomes out of the question because the oncoming flow is fully developed. For general pipe flows it seems not unlikely that the upstream influence is then largely confined to a distance upstream that is comparable with the typical pipe width (cf. Smith 1976*a*, *b*). For channel flows, however, Smith (1976*b*) has shown that a small asymmetric disturbance at the walls can generate a large-scale upstream effect, causing the motion to split up into essentially three regions. These regions are a core motion, involving small inviscid perturbations to the oncoming Poiseuille flow, and two viscous nonlinear wall layers, where the flow is driven by the induced pressure gradient and crucially affected by the displacement of the core. The upstream influence remains insignificant unless the height of the indentation, for example, is as large as $K^{-\frac{3}{7}}$ relative to the channel width a, in which case the flow is affected appreciably at large distances $[O(aK^{\frac{1}{7}})]$ upstream and separation is likely to occur there. (A linearized analysis by Smith (1976*b*) confirms these trends.) Increasing the size of the disturbance then presumably forces the separation point further upstream and generally causes an increase in the size of the upstream response. Consequently we are led to the contention that, when the height of the asymmetric indentation is even greater than this order of magnitude, the necessary adjustment of the flow upstream must involve all or part of the underlying structure of the free interaction induced by a relative height $K^{-\frac{2}{7}}$. In other words, a deviation from the oncoming flow is most likely to occur first at a distance $O(aK^{\frac{1}{7}})$ ahead of the particular distortion. (This implies that Wilson's (1969) conclusions on upstream influence are incomplete.) Hence, for the problem of motion through a channel whose width is altered sharply, asymmetrically and by a finite amount, at some point, the flow responds by initiating a nonlinear free interaction far upstream. This interaction can be expected to alter the flow properties substantially even before the obstacle is reached, and must be such that the fluid can then pass through the constriction or dilation.

The orders of magnitude of the velocities and pressure, and the critical length

scale on which the upstream adjustment occurs, are determined in § 2 below and the formal asymptotic expansion of the solution for $K \gg 1$ is set down in § 3. The upstream response is found to be due to the pressure gradient acting across the channel, which is induced by the slight displacement of the core. For, if the pressure perturbation near one wall is positive, the viscous layer there tends to thicken. So the other wall layer thins to conserve the mass flux, and the transverse momentum thus produced generates a transverse pressure gradient. The pressure near the second wall then turns out to be of opposite sign and consequently tends to accentuate the compression of the second wall layer, sustaining the interaction process. The ensuing development of the flow is nonlinear and the necessary numerical solution, an integration of the two wall layers simultaneously to calculate the pressure and core displacement, is described in § 4. Separation is found to occur in a regular fashion in one of the layers but downstream the compression of the other layer starts to dominate the motion, and the numerical results point to the occurrence of a singularity at a finite distance (on the long, free-interaction, scale) beyond separation. An analysis of the ultimate structure of the free interaction, based on the existence of such a singularity and presented in § 5, is apparently self-consistent when a self-similar form is assumed in the reversed flow zone, and despite the arbitrariness (due to the features of the flow upstream) in the local solution there comparison of the theory with the calculations indicates general agreement. The implications for the motion even nearer the severe disturbance, i.e. at distances upstream that are comparable with the channel width, are discussed in § 6.

The overall conclusion is that the flow at one wall must separate at a large distance ($= 0{\cdot}49aK^{\frac{1}{7}}$) upstream. Consequently, and contrary to the often-conjectured model of flow ahead of a finite indentation, say, the separation streamline does not leave the wall at a finite angle but at an angle that tends to zero as the Reynolds number tends to infinity. While still at finite distances from the disturbance, the flow has already evolved a nonlinear character quite distinct from that of the original Poiseuille flow. Thus the local motion at finite distances from the particular asymmetric disturbance does not join smoothly on to the original Poiseuille form but instead is a continuation of the ultimate form of the long-scale interaction. Qualitative and quantitative comparisons (§ 6) with numerical solutions of the full Navier–Stokes equations tend to bear out the existence of this long-scale upstream adjustment in asymmetric flows.

We emphasize that our concern here is with finite asymmetric disturbances (and with laminar flow). The nonlinear upstream interaction outlined above would not occur in a finite symmetric case, and the necessary upstream adjustment in such a case remains undetermined by this work.

2. Non-dimensionalization and the critical length scale

Letting $-g$ ($g > 0$) denote the pressure gradient dp^*/dx^* driving the flow far upstream in the channel, we write the pressure as $agp(x, y)$, where a is the channel width and $x^* = ax$ and $y^* = ay$ signify distances downstream and across the channel, respectively, from an origin fixed in the lower wall ($y = 0$) of the un-

disturbed channel. The velocities $a^2g\rho^{-1}\nu^{-1}(u,v)$ in the (x,y) directions then satisfy the non-dimensional Navier–Stokes equations

$$\operatorname{div}\mathbf{u} = 0, \quad K(\mathbf{u}\cdot\nabla)\mathbf{u} = -\nabla p + \nabla^2\mathbf{u}, \tag{2.1}$$

in the usual notation, $\mathbf{u} = (u,v)$ being zero on the walls $y = 0,1$ upstream of any change in the boundary conditions. The Reynolds number K here is defined by

$$K = ga^3/\rho\nu^2, \tag{2.2}$$

ρ and ν standing for the density and kinematic viscosity of the fluid, and we assume henceforth that $K \gg 1$. Far upstream the motion is supposed to have the fully developed Poiseuille form

$$u = \tfrac{1}{2}(y-y^2) \equiv U_\infty(y), \quad v = 0, \quad p = p_0 - x, \tag{2.3}$$

where p_0 is an $O(1)$ constant.

Smith (1976*a*, *b*), in studying the effects of small constrictions on channel flow, has already demonstrated the importance of the regime $\alpha \sim K^{-\frac{3}{7}}$, where α represents the typical asymmetric deviation of the slope of the channel wall from its undisturbed direction. The following order-of-magnitude considerations show how the critical scalings of the velocities, pressures and lengths involved are derived for the free interaction which takes place far ahead of a constriction even when that constriction is not small. (An alternative derivation of the scalings and structure of the solution emerges from an examination of the initial character of the solution to a corner problem when $\alpha \sim K^{-1}$, or of the flow at a junction of two channels, when analysed according to conventional boundary-layer theory. Results (2.8) below follow in much the same way as those Stewartson (1969) and Messiter (1970) deduced for the structure of the triple deck close to the trailing edge of a flat plate in a uniform external stream.) The theory that we put forward for the upstream interaction here is founded on the notion that such an interaction in an asymmetric channel takes place chiefly because of the generation of a significant transverse pressure gradient in the main inviscid core of the fluid. The core motion involves a simple inviscid but rotational displacement of the oncoming Poiseuille motion (2.3), but since the velocity in (2.3) reduces to zero at the walls the displacement induces viscous interactions in thin layers near both walls. On the other hand, the pressure at a given station downstream takes a value in the layer at the top wall different from that in the lower layer because of its transverse variation in the core, and it is this difference that is the cause of the self-sustaining interaction between the two pressures and the displacement effect.

Thus in the core flow the stream function $\psi(x,y)$, defined by $u = \partial\psi/\partial y$, $v = -\partial\psi/\partial x$ and $\psi(-\infty,0) = 0$ (so that $\psi(-\infty,y) = \frac{1}{4}y^2 - \frac{1}{6}y^3 \equiv \psi_\infty(y)$, say), is effectively

$$\psi = \psi_\infty(y + \delta A(X)). \tag{2.4}$$

Here the displacement function $A(X)$ is a function of $X = x/\Delta$ to be determined and the unknown critical streamwise length scale Δ is supposed to be $\gg 1$. The unknown perturbation parameter $\delta \ll 1$ represents the thicknesses of the viscous wall layers, which therefore perturb the Poiseuille flow by the same amount.

The continuity and streamwise momentum equations are then satisfied to leading order provided that $\lambda \ll \delta K$, which is justified *a posteriori*. λ signifies the unknown order of magnitude of the pressure force, but the transverse momentum equation gives

$$\partial p/\partial y = U_\infty^2(y)\, A''(X)\, (K\delta/\lambda\Delta^2), \tag{2.5}$$

where a prime is used to denote differentiation with respect to the assigned independent variable. As the bottom wall is neared the solution (2.4) is rendered invalid when $y \sim \delta$, however, and there viscous resistances must play a major role, implying in the x momentum equation the balances

$$\frac{K\delta^2}{\Delta} = \frac{\lambda}{\Delta} = \frac{1}{\delta} \tag{2.6}$$

since u is now $O(\delta)$. The same balances of orders arise in the top-wall viscous layer of thickness $\sim \delta$. The final requirement that fixes the characteristic scales Δ, δ and λ is that

$$K\delta/\lambda\Delta^2 = 1, \tag{2.7}$$

which allows the transverse pressure gradient $\partial p/\partial y$ to be non-zero. From (2.6) and (2.7) we then obtain the crucial orders of magnitude

$$\Delta = K^{\frac{1}{7}}, \quad \delta = K^{-\frac{2}{7}}, \quad \lambda = K^{\frac{3}{7}} \tag{2.8}$$

for the x length scale, the thicknesses of the two viscous layers and the pressure distribution.

Since the ratio of the y length scale to the x length scale is $K^{-\frac{3}{7}}$, it follows that if the disturbance to the shape of the wall is of typical inclination $\alpha \ll K^{-\frac{3}{7}}$ then $\partial p/\partial y \ll 1$, the free interaction that is found to develop under (2.8) is not substantial and a linearized solution is possible. This was the situation that Smith (1976*a*, *b*) concentrated on but his work also elucidated the importance of the pressure variation $\partial p/\partial y$. From (2.5)–(2.8) and Smith's work we may conclude that if $\alpha \sim K^{-\frac{3}{7}}$ the interaction will be nonlinear and a computational task will be set, with flow separation likely to occur on one of the walls near the start of the indentation, and that as α increases beyond $O(K^{-\frac{3}{7}})$ the separation point will be pushed further and further upstream. Our interest is almost wholly in the second case, where the flow gradually develops away from the Poiseuille form long before the actual indentation (or other asymmetric disturbance) is reached. It is shown below that the *free* interaction, occurring when (2.8) holds and the Poiseuille motion upstream is slightly perturbed, in fact explains the nature of the motion upstream in the most physically interesting situation, i.e. where α is $O(1)$.

The formal expansion procedure stemming from the scalings (2.8) is set out in § 3 below for the three regions of flow. Section 4 is then devoted to a description of the necessary numerical approach and its results, which give the structure of the flow field as the assumed indentation downstream is approached, both on the long $[O(aK^{\frac{1}{7}})]$ length scale (studied in § 5) and on the $O(a)$ length scale (see § 6).

3. The three regions of flow

Since powers of $K^{-\frac{1}{7}}$ are involved it is convenient to use the parameter

$$\epsilon = K^{-\frac{1}{7}} \quad (\ll 1), \tag{3.1}$$

so that in general the solution is expected to proceed in integral powers of ϵ (and $\ln \epsilon$), according to § 2. Then the postulate is that, on a critical length scale defined where the streamwise co-ordinate

$$X = \epsilon x \tag{3.2}$$

is $O(1)$, the flow subdivides into a core motion I for $0 < y < 1$ and two viscous layers II and III arising for y and $1-y$ of order ϵ^2 respectively.

Starting with region I, we expand the solution in the form

$$\left.\begin{aligned} u &= U_\infty(y) + \epsilon^2 u_1(X,y) + \epsilon^4 u_2(X,y) + O(\epsilon^6), \\ v &= \epsilon^3 v_1(X,y) + \epsilon^5 v_2(X,y) + O(\epsilon^7), \\ p &= \epsilon^{-3} p_1(X,y) + \epsilon^{-1} p_2(X,y) + O(1). \end{aligned}\right\} \tag{3.3}$$

From substitution into the equations of continuity and x momentum in (2.1), and neglecting terms of relative order ϵ^2, the solutions for the perturbations u_1 and v_1 that merge with the upstream solution (2.3) as $X \to -\infty$ are then (Stewartson & Williams 1969)

$$u_1 = A(X)\, U'_\infty(y), \quad v_1 = -A'(X)\, U_\infty(y), \tag{3.4}$$

with $A(-\infty) = 0$. The y momentum equation then yields effectively (2.5) to first order, so that, on integration with respect to y,

$$p_1(X,y) = P(X) + A''(X) \int_0^y U_\infty^2(t)\, dt, \tag{3.5}$$

where $P(X) = p_1(X,0)$ is a function of X to be determined, with $P(-\infty) = 0$. We postulate that the functions $A(X)$ and $P(X)$ are non-zero and so to first order the solution (3.4) represents a wholesale displacement of the oncoming streamlines by an amount $-A(X)$, accompanied by the pressure variation (3.5) across the channel. Hence as $y \to O(\epsilon^2)$ the expansion (3.3) becomes inaccurate since $U_\infty(y)$ ($\approx \frac{1}{2}y$) tends to zero whereas u_1 ($\approx \frac{1}{2}A(X)$) is non-zero, and the lower viscous layer II is thereby invoked. Similarly, the upper viscous layer III is necessary as $y \to 1$. The subsequent perturbations in (3.3) confirm these trends but lead also to the logarithmic behaviour in (3.6) and (3.8) below.

In II we set $y = \epsilon^2 Y$, where Y is an order-one co-ordinate, and express the flow properties as

$$\left.\begin{aligned} u &= \epsilon^2 U(X, Y) + O(\epsilon^4 \ln \epsilon), \\ v &= \epsilon^5 V(X, Y) + O(\epsilon^7 \ln \epsilon), \\ p &= \epsilon^{-3} P_1(X, Y) + O(\epsilon^{-1} \ln \epsilon) \end{aligned}\right\} \tag{3.6}$$

owing to the expansion (3.3) and the solutions (3.4) and (3.5). The Navier–Stokes equations then show, to $O(\epsilon^{-5})$ in the y momentum equation, that P_1 is independent of Y. Hence $P_1 = P(X)$, to assure compatibility with (3.5) at $y = 0$, and to

$O(\epsilon^3)$ and $O(\epsilon^{-2})$ in the continuity and x momentum equations respectively the boundary-layer equations

$$\frac{\partial U}{\partial X}+\frac{\partial V}{\partial Y}=0, \quad U\frac{\partial U}{\partial X}+V\frac{\partial U}{\partial Y}=-\frac{dP}{dX}+\frac{\partial^2 U}{\partial Y^2} \tag{3.7a}$$

are the governing equations for II. The boundary conditions become

$$\left.\begin{aligned} U=V=0 \quad \text{at} \quad Y=0, \quad U\sim\tfrac{1}{2}(Y+A(X)) \quad \text{as} \quad Y\to\infty, \\ U\sim\tfrac{1}{2}Y \quad \text{as} \quad X\to-\infty \end{aligned}\right\} \tag{3.7b}$$

from the no-slip constraint at the wall, from matching with I as $Y\to\infty$ and from continuation with the Poiseuille solution ($U=\frac{1}{2}Y$, $V=P=A=0$) far upstream. Boundary and matching conditions and linear equations may be written down for the lower-order terms of (3.6), but the essential problem of region II, (3.7*a*, *b*), is clearly insufficient to determine the induced pressure force $P(X)$ and displacement function $A(X)$ driving the flow. In addition it is necessary to consider the upper viscous layer III that borders the wall $y=1$.

With the appropriate normal co-ordinate $Z=\epsilon^{-2}(1-y)$ defining the wall layer III, the solution is expanded in similar fashion to (3.6):

$$\left.\begin{aligned} u&=\epsilon^2\tilde{U}(X,Z)+O(\epsilon^4\ln\epsilon), \\ v&=-\epsilon^5\tilde{V}(X,Z)+O(\epsilon^7\ln\epsilon), \\ p&=\epsilon^{-3}\tilde{P}(X)+O(\epsilon^{-1}\ln\epsilon). \end{aligned}\right\} \tag{3.8}$$

Here the result $\partial\tilde{P}/\partial Z=0$ from the transverse momentum equation has been anticipated. As in II the controlling equations for III are the boundary-layer equations

$$\frac{\partial\tilde{U}}{\partial X}+\frac{\partial\tilde{V}}{\partial Z}=0, \quad \tilde{U}\frac{\partial\tilde{U}}{\partial X}+\tilde{V}\frac{\partial\tilde{U}}{\partial Z}=-\frac{d\tilde{P}}{dX}+\frac{\partial^2\tilde{U}}{\partial Z^2}, \tag{3.9a}$$

where

$$\tilde{P}(X)=P(X)+\tfrac{1}{120}A''(X), \tag{3.9b}$$

subject to the boundary conditions

$$\left.\begin{aligned} \tilde{U}=\tilde{V}=0 \quad \text{at} \quad Z=0, \quad \tilde{U}\sim\tfrac{1}{2}(Z-A(X)) \quad \text{as} \quad Z\to\infty, \\ \tilde{U}\sim\tfrac{1}{2}Z \quad \text{as} \quad X\to-\infty. \end{aligned}\right\} \tag{3.9c}$$

Here the induced pressure $\tilde{P}(X)$ in III is fixed by matching the pressure with that in I at the edge of the upper layer, and the boundary conditions (3.9*c*) follow as in II.

The fundamental problem of the three-layer system is therefore to solve (3.7*a*, *b*) and (3.9*a*–*c*) simultaneously, with the pressure $P(X)$ and displacement $A(X)$ unknown. Clearly one solution of this system is $U=\frac{1}{2}Y$, $\tilde{U}=\frac{1}{2}Z$, $V=\tilde{V}=P=\tilde{P}=A=0$, which means that the Poiseuille flow continues undisturbed. However, Smith (1976*b*) showed that in the solution for $X\to-\infty$ there is an apparent non-uniqueness (the non-uniqueness is resolved by the downstream conditions) and another motion is possible which gradually evolves away from the Poiseuille form. For X large and negative, the pressure in II is small and from (3.7)–(3.9) must be given by

$$P(X)\approx b_1 e^{\theta X}+O(e^{2\theta X}). \tag{3.10}$$

The entire flow can then be described as a small perturbation of the Poiseuille solution, the magnitude of the perturbation being dependent solely on the unknown constant b_1. The perturbation solutions and the constant θ can be determined by the need for consistency between the disturbances in II and III, as follows. In II

$$\left.\begin{aligned} U &\approx \tfrac{1}{2}Y - b_1 e^{\theta X} f_1'(Y) + O(e^{2\theta X}), \\ V &\approx b_1 \theta e^{\theta X} f_1(Y) + O(e^{2\theta X}), \end{aligned}\right\} \tag{3.11}$$

and with terms $O(e^{2\theta X})$ in (3.7a, b) neglected, the solution for $f_1(Y)$ gives the condition

$$\beta_1/2b_1 = 2^{\frac{2}{3}}\theta^{\frac{1}{3}}/3\,\mathrm{Ai}'(0), \tag{3.12}$$

where

$$A(X) \approx \beta_1 e^{\theta X} + O(e^{2\theta X}). \tag{3.13}$$

The constant β_1 is to be found in terms of b_1, and Ai is the Airy function. Similarly in III the expansion

$$\left.\begin{aligned} \tilde{U} &\approx \tfrac{1}{2}Z - b_1 e^{\theta X} \tilde{f}_1'(Z) + O(e^{2\theta X}), \\ \tilde{V} &\approx b_1 \theta e^{\theta X} \tilde{f}_1(Z) + O(e^{2\theta X}) \end{aligned}\right\} \tag{3.14}$$

holds and solution for the function $\tilde{f}_1(Z)$ satisfying the constraints at $Z = 0$ and as $Z \to \infty$ yields

$$\frac{\beta_1}{2b_1} = -\frac{2^{\frac{2}{3}}\theta^{\frac{1}{3}}}{3\,\mathrm{Ai}'(0)}\left(1 + \frac{\theta^2\beta_1}{120b_1}\right) \tag{3.15}$$

since the pressure in III is $(b_1 + \frac{1}{120}\theta^2\beta_1)\,e^{\theta X}$ approximately. Eliminating $\beta_1/2b_1$ between (3.12) and (3.15) therefore gives the value of θ as

$$\theta = 2[-45\,\mathrm{Ai}'(0)]^{\frac{3}{7}} = 5{\cdot}731\ldots, \tag{3.16}$$

so that $\beta_1 = -240b_1\theta^{-2}$ and only the constant b_1 remains undetermined. For a problem such as the determination of the flow through the channel when the lower wall is distorted into the shape $Y = hF(X)$, where the constant $h \sim 1$ and $F(\pm\infty) = 0$, the value of b_1 would be fixed by the requirement that the flow should also return to the Poiseuille form far downstream. A shooting method, akin to that used in triple-deck calculations (Stewartson 1970; Smith & Stewartson 1973), would be called for. We are interested instead in the nature of the free interaction alone and hence wish to discover the ensuing nonlinear development of the flow in II and III when the motion upstream is slightly disturbed, as in (3.10)–(3.16), but when the no-slip conditions at $Y = Z = 0$ are satisfied throughout. Thus our approach is analogous to that of Stewartson & Williams (1969) and Stewartson (1970), who considered, respectively, small positive and negative values of the induced pressure perturbation in their fundamental problems. However, in contrast with their work, where the positive and negative upstream disturbances produced quite distinct downstream solutions, in our study there is effectively only one form of free interaction. If $b_1 > 0$ then initially in II the pressure rises and the skin friction $\tau(X) = (\partial U/\partial Y)_{Y=0}$ falls from the undisturbed value 0·5 (see Smith 1976*b*) as the displacement $-A(X)$ rises, while in III the pressure drops, the skin friction $\tilde{\tau}(X) = (\partial\tilde{U}/\partial Z)$ $(Z = 0)$ increases and the displacement effect for III, i.e. $+A(X)$, decreases. In physical terms, the small increase in pressure near the lower wall causes the viscous layer there to expand,

and consequently the upper layer to contract, a motion which sets up a negative pressure gradient across the channel. This produces a small decrease in pressure near the upper wall, tending to induce an even greater compression of the viscous layer there, and so the process is reinforced. If $b_1 < 0$ the roles of II and III are simply interchanged. Hence the case $b_1 > 0$ covers both situations and we can expect that as X increases from $-\infty$ the lower layer II will continue its trend towards separation whereas as in III the flow will be increasingly compressed. One of the major questions then concerns the ultimate behaviour of this free interaction. Does the solution steadily evolve an asymptotic separated structure as $X \to \infty$, as in Stewartson & Williams (1969, 1973), or is it dominated by a singularity at a finite value of X (cf. Stewartson 1970)? The answer, and an appreciation of the nonlinear evolution of the motion, necessitates a numerical integration of the equations dictating the flow in the lower and upper viscous zones, which is described in the next section.

4. Numerical results

To study the nonlinear behaviour that develops from the small perturbation to the Poiseuille solution a numerical approach similar to that used by Smith & Stewartson (1973) and Smith (1974) (see also Keller & Cebeci 1971) was adopted. The governing equations (3.7*a*) and (3.9*a*) of II and III were expressed as first-order equations by setting

$$\left.\begin{aligned} s = \partial\Psi/\partial Y, \quad t = \partial s/\partial Y \quad \text{in II,} \\ c = \partial\tilde{\Psi}/\partial Z, \quad e = \partial c/\partial Z \quad \text{in III,} \end{aligned}\right\} \tag{4.1}$$

where $\Psi(X, Y)$ and $\tilde{\Psi}(X, Z)$ are the stream functions in II and III ($U = \partial\Psi/\partial Y$, $V = -\partial\Psi/\partial X$, $\tilde{U} = \partial\tilde{\Psi}/\partial Z$ and $\tilde{V} = -\partial\tilde{\Psi}/\partial X$ with $\Psi(X, 0) = \tilde{\Psi}(X, 0) = 0$). Thus

$$\left.\begin{aligned} \Psi &\sim \tfrac{1}{4}(Y + A(X))^2 + 2P(X) \quad \text{as} \quad Y \to \infty, \\ \tilde{\Psi} &\sim \tfrac{1}{4}(Z - A(X))^2 + 2P(X) + \tfrac{1}{60}D(X) \quad \text{as} \quad Z \to \infty \end{aligned}\right\} \tag{4.2}$$

from analysis of the solutions to (3.7*a*) and (3.9*a*) for $Y \gg 1$ and $Z \gg 1$ respectively; here we have introduced the function $D(X) = B'(X) = A''(X)$. Layers II and III are represented respectively by J and K mesh points spaced at distances h and $\tilde{h}$ apart across each layer. Given the solution at a particular X station, (3.7*a*), (3.9*a*) and (4.1), applied in discrete form, provide $3J + 3K - 6$ equations for the $3J + 3K + 4$ unknowns, namely B, D, A, P and the values of Ψ, s, t, $\tilde{\Psi}$, c and e at each mesh point, at the next station downstream. The no-slip constraints together with (4.2) and its Y and Z derivatives yield eight more relations and the final two discrete first-order relations are those between B, D and A. The solution can then be advanced forward safely in the X direction, provided that U and $\tilde{U}$ remain positive (see below, however), the $3J + 3K + 4$ nonlinear equations being solved iteratively, with a tolerance q between successive iterates setting the criterion for convergence to the solution at each station.

The calculations were usually initiated by perturbing the pressure P by a small amount $P_{-\infty}$ but with the undisturbed solutions for the velocities. Typically the values $P_{-\infty} = 10^{-4}$ and $q = 10^{-7}$ were chosen, and a step length $\Delta x = 0{\cdot}01$

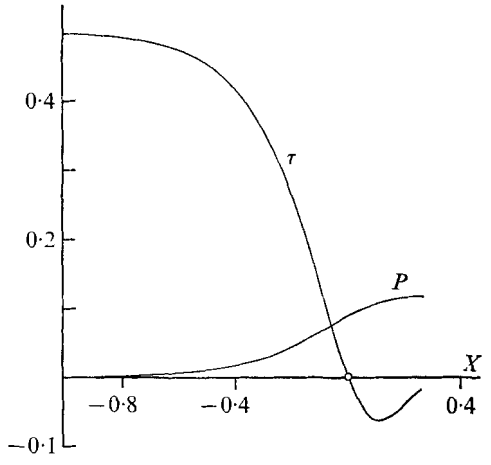

FIGURE 1. Solutions for P and $\tau = (\partial U/\partial Y)_{Y=0}$ as functions of X.

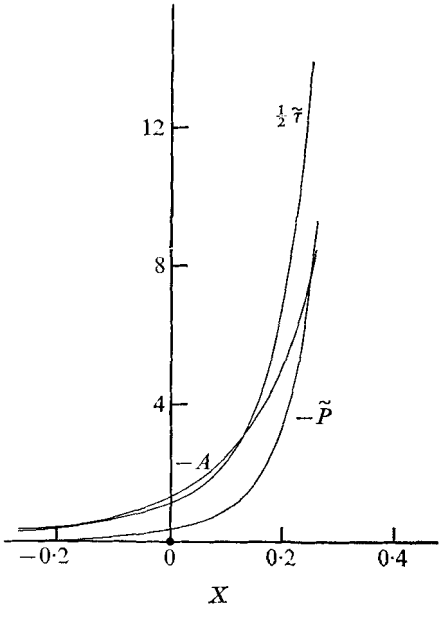

FIGURE 2. Plots of A, $\tilde{\tau} = (\partial \tilde{U}/\partial Z)_{Z=0}$ and $\tilde{P} = P + \frac{1}{120}A''$ *vs.* X.

in the x direction and mesh widths $h = 0{\cdot}1$ and $\tilde{h} = 0{\cdot}02$ in II and III. These values, and those of J and K (typically 100), were selected because of the nature of both the initial form (3.10)–(3.16) and the terminal form (see § 5) of the free interaction. Tests of the proposed second-order accuracy of the method proved favourable and as expected the choice of a different value, 5×10^{-6}, for $P_{-\infty}$ merely provoked an effective shift in the origin for X.

Some of the results obtained during the calculations are summarized in figures 1–4. As X is increased from its initial value $X = X_{-\infty}$ the skin friction $\tau(X)$ in the lower layer II continues to fall and the pressure $P(X)$ to rise (see

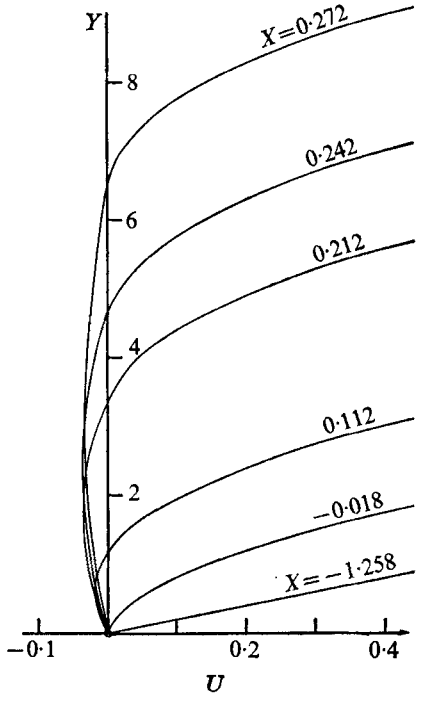

FIGURE 3. Velocity profiles in the separating layer II of the free interaction: $X_{-\infty} = -1{\cdot}258$.

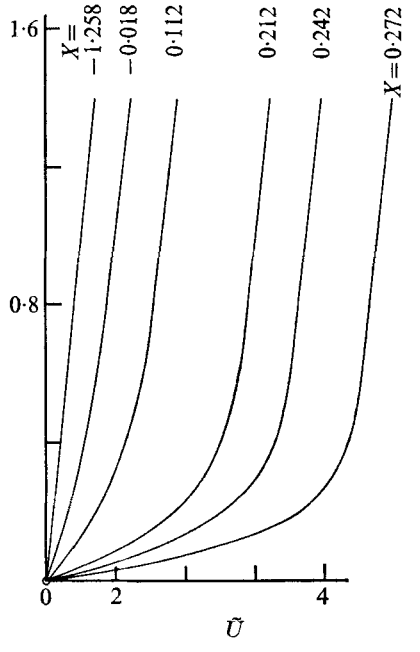

FIGURE 4. Some profiles of $\tilde{U}$ in layer III: $X_{-\infty} = -1{\cdot}258$.

$X-X_{-\infty}$	$-A$	$\tilde{\tau}$	$\tilde{\tau}_1$	P	$-\tau$	$-U_{\min}$
(0	0	0·5	0·5	0	−0·5	0)
1·43	3·737	8·622	0·5485	0·11416	0·0547	0·0319
1·45	4·326	10·81	0·5306	0·11495	0·0479	0·0346
1·47	5·044	13·79	0·5169	0·11552	0·0409	0·0363
1·49	5·932	17·92	0·5089	0·11591	0·0340	0·0354
1·51	7·051	23·82	0·5037	0·11617	0·0275	0·0343
1·53	8·491	32·50	0·5012	0·11634	0·0224	0·0320

TABLE 1. Sample values of $A, \tilde{\tau}, \tilde{\tau}_1, P, \tau$ and $U_{\min}$ on nearing the end of the integration range ($\tilde{\tau}_1 = \partial\tilde{U}(X,1)/\partial Z$, $U_{\min}$ = minimum value of U, $X_{-\infty} = -1{\cdot}258$).

figure 1), initially according with the behaviours indicated in (3.10)–(3.16). The displacement $A(X)$ and pressure $P(X)+\frac{1}{120}D(X) = \tilde{P}$ in layer III both continue to decrease and the skin friction $\tilde{\tau}(X)$ rises increasingly, as shown in figure 2. Separation of the flow in II ($\tau = 0$) is eventually reached, with $P = P_s = 0{\cdot}0909$ and $A = A_s = -1{\cdot}275$ (and for definiteness we take the separation point to be the origin for X), and it appears to be a regular phenomenon. The Goldstein (1948) singularity that arises in classical boundary-layer theory at separation is absent here by a reasoning similar to that of Stewartson & Williams (1969) and Stewartson (1974), since the displacement and pressure are intimately related and must adjust their values at separation to ensure a regular solution. In brief, a singularity in τ would provoke a singularity in A, and hence a much worse singularity in D, which cannot be consistent with the assumptions of the Goldstein singularity structure. Beyond separation, despite the problems of non-uniqueness (see also § 5 below) posed by the upstream-moving part of the flow in II, the solutions obtained by simply allowing the calculations to proceed without modification in $X > 0$ seemed to be physically reasonable. The shear stress $\tau(X)$ attains a negative minimum and then starts to increase slowly and the pressure curve in II gradually flattens out. In the upper layer III the pressure and displacement continue their downward (and the wall shear stress its upward) plunge. The comparative smallness of the backward velocities in II suggested the alternative use of the Reyhner & Flügge-Lotz (1968) approach of neglecting $U\partial U/\partial X$ when $U < 0$. This was also applied but the results differed little from those shown.

Graphs of the velocity profiles in regions II and III are drawn in figures 3 and 4 for various values of X. It is seen that in III the fluid is pressed increasingly onto the wall $Z = 0$ and that the part of III where the shear differs significantly from 0·5 becomes ever smaller. In II the flow features suggest that a downstream structure analogous to that of Stewartson & Williams (1973) might emerge as $X \to \infty$. For, after reversed flow sets in at $X = 0$, the viscous effects begin to concentrate around the detached streamline $\Psi = 0$, beneath which the reversed flow velocities and shear are relatively small, and above which the shear attains its edge value 0·5 quite rapidly, and this is essentially the phenomenon described by Stewartson & Williams. However, the results for $\tilde{\tau}(X)$, $\tilde{P}(X)$ and $A(X)$ indicate firmly that such a form is highly unlikely and instead point to the occurrence of a singularity at a finite value of X ($X = X_0$, say), downstream of

separation, beyond which the solution cannot be continued. Table 1 and figures 5 and 6 below, taken at their face value, bear out this assertion. We show in the next section that an asymptotic description of the solution as

$$\bar{X} = X_0 - X \to 0+$$

may be constructed which appears to be self-consistent and broadly in line with the calculated results, as far as the latter could be taken without divergence, near the singular point $X = X_0$.

5. The ultimate structure of the free interaction

First, in the upper viscous region III the nature of the singularity is similar to that discussed by Stewartson (1970), the shearing flow being virtually unaffected until the wall itself is almost reached, so that a thin slip layer is induced. To find the exact details of the compression here we seek in the slip layer, assuming it to have thickness $\propto \bar{X}^n$, a similarity solution wherein $\tilde{\Psi}\bar{X}^m$ is a function of $\eta = Z\bar{X}^{-n}$ (~ 1), m and n being unknown powers. The equation of motion (3.9a) then requires that $n = m+1$ and that if the pressure $\sim \bar{X}^l$ (l unknown) then also $l = 1-m-3n$. But the strong favourable pressure gradient in III is dominated by its $D'(X) = A'''(X)$ component, implying $A(X) \sim \bar{X}^{l+2}$. Also the streamwise velocity in the slip layer matches on to the displacement effect $A(X)$ in (3.9a), since Z is small, and hence $m+n+l = -2$ is required. Therefore, for this structure to hold, it is necessary that $m = \frac{1}{2}$, $n = \frac{3}{2}$ and $l = -4$, and the solution in the slip layer takes the form

$$\tilde{\Psi} = \bar{X}^{-\frac{1}{2}} F_0(\eta), \quad \eta = Z/\bar{X}^{\frac{3}{2}}, \tag{5.1}$$

to first order, with

$$A(X) \approx -A_0/\bar{X}^2, \quad P(X) \approx P_0 + o(1). \tag{5.2}$$

Here A_0 and P_0 are constants to be determined (the influence of P_0 is discussed later). Substitution into (3.9a) gives the equation

$$F_0''' + \tfrac{1}{2} F_0 F_0'' - 2F_0'^2 = -\tfrac{1}{5} A_0 \tag{5.3}$$

for the function $F_0(\eta)$. However $\partial\tilde{\Psi}/\partial Z \to A(X)$ as $\eta \to \infty$, which imposes the condition $F_0'(\infty) = (\frac{1}{10}A_0)^{\frac{1}{2}}$, from (5.2). So the above equation for F_0 yields the value

$$A_0 = \tfrac{2}{5} \tag{5.4}$$

and $F_0(\eta)$ satisfies the Falkner–Skan equation (5.3), with $F_0(0) = F_0'(0) = 0$ and $F_0'(\infty) = \frac{1}{5}$. Numerical solution gives

$$F_0''(0) = 0{\cdot}1488, \quad \beta_0 \equiv \lim_{\eta\to\infty} (F_0 - \tfrac{1}{5}\eta) = -0{\cdot}2341. \tag{5.5}$$

Second, the above behaviour in III must be compatible with the partly reversed motion in the lower layer II as $\bar{X} \to 0$. A three-zone framework for the solution in II, similar to that studied by Stewartson & Williams (1973), with the vorticity variation largely confined to the neighbourhood of the free shear layer centred around $Y = -A(X)$, would be implied if P_0 were zero. For then the outer

shearing flow pulling the detached layer forwards would be $\Psi \sim \frac{1}{4}\bar{Y}^2 + o(1)$ [from (3.7*b*)], where $\bar{Y} = Y + A(X)$. But it is manifestly true from the computed results that $P_0 > 0$. Indeed, a zero value for the pressure $P(X)$ at $\bar{X} = 0$ would suggest a reattachment of layer II before $X = X_0$ since the driving pressure gradient would become favourable, albeit 'at the last moment', a phenomenon seemingly unreasonable from a physical standpoint. It can be shown that such a three-zone treatment cannot hold therefore. For, if P_0 is non-zero and the outer shear continues to describe the solution down to the detached vorticity layer, then the stream function takes the value $2P_0 + O(1)$ throughout that layer. The comparatively slow, reversed, flow underneath is driven by a small pressure gradient, which must be adverse, and the relevant Falkner–Skan equation governing the slow flow is found to have no solution.

We believe that this difficulty is due entirely to the indeterminacy associated with the fluid properties upstream and not to the effect of the backward-moving fluid beneath the vorticity layer. Because the fluid in and below the vorticity layer is all slowing down as $X \to X_0-$, the indeterminacy is then able to affect not only the reversed flow but also the whole forward-moving part of II above the detached layer, even to first order in $\bar{X}$. By contrast, in Stewartson & Williams' (1973) situation the velocities in and above the detached layer are increasing far downstream. So there the arbitrariness, again associated with the influence of the solution upstream, is basically a lower-order effect and, with a self-similar structure assumed, the asymptotic solution is then uniquely determined to first order, apart from a multiplicative constant below the shear layer. More precisely in our problem, we propose that an adjustment of the flow from its outer shear in (3.7*b*) has to take place above the shear layer and, assuming a self-similar character to be the most physically realistic (see § 6), the asymptotic structure of the separating layer II as $X \to X_0-$ consists essentially of four regions (i)–(iv) (see figure 5 below), described as follows.

Starting with region (iv), which lies above the detached layer and in which $\bar{Y}$ is positive and of order unity, we have to admit a non-uniqueness into the solution for the stream function immediately. For purely local considerations demand only that the final velocity profile at $X = X_0$ takes a forward-moving form compatible with the outer condition of (3.7*b*) and with a matching condition as the vorticity layer is approached. Thus, for $0 \leqslant \bar{X} \ll 1$ with $\bar{Y}$ order one, the expansion

$$\Psi = \mathscr{F}_0(\bar{Y}) + \bar{X}\mathscr{F}_1(\bar{Y}) + O(\bar{X}^2) \tag{5.6}$$

will satisfy the controlling equations and boundary conditions of II provided that the functions $\mathscr{F}_0(\bar{Y})$ and $\mathscr{F}_1(\bar{Y})$ satisfy

$$\mathscr{F}_0(\bar{Y}) \sim \frac{\bar{Y}^2}{4} + 2P_0 \quad \text{as} \quad \bar{Y} \to \infty, \quad \mathscr{F}_1(\bar{Y}) = -\mathscr{F}_0'(\bar{Y}) \int_\infty^{\bar{Y}} \frac{\mathscr{F}_0'''(t)}{\mathscr{F}_0'(t)^2}\, dt \tag{5.7}$$

and, further, $dP/dX \ll 1$. To join this to the solution within the vorticity layer (iii) centred about $\bar{Y} = 0$ we must also impose $\mathscr{F}_0(0) = 0$ and so the profile $\mathscr{F}_0 = \frac{1}{4}\bar{Y}^2 + 2P_0$ will not suffice, but still $\mathscr{F}_0(\bar{Y})$ remains undetermined. If we suppose that

$$\mathscr{F}_0(\bar{Y}) \sim \kappa_0 \bar{Y}^2 + \kappa_1 \bar{Y}^3 + \kappa_2 \bar{Y}^4 + \ldots \quad \text{as} \quad \bar{Y} \to 0, \tag{5.8}$$

which gives a physically sensible profile, with the coefficients κ_i unspecified, then for $\bar{Y} \ll 1$

$$\mathscr{F}_1(\bar{Y}) \sim 3\kappa_1/\kappa_0 + O(\bar{Y}) \tag{5.9}$$

provided that $\kappa_0 \neq 0$. *Hence, in (iii), which being viscous has thickness* $O(\bar{X}^{\frac{1}{3}})$, so that $\xi = \bar{Y}/\bar{X}^{\frac{1}{3}}$ is order one, we have the solution

$$\Psi = \bar{X}^{\frac{2}{3}} G_0(\xi) + O(\bar{X}), \tag{5.10}$$

where, from (3.7*a*), the function $G_0(\xi)$ is governed by

$$G_0''' - \tfrac{2}{3} G_0 G_0'' + \tfrac{1}{3} G_0'^2 = 0. \tag{5.11a}$$

The upper boundary conditions for (iii) are those of merging with the form of (iv) as $\bar{Y} \to 0$ there, implying

$$G_0 - \kappa_0 \xi^2 \to 0 \quad \text{as} \quad \xi \to \infty, \tag{5.11b}$$

while as $\xi \to -\infty$ we require G_0 to remain bounded since the motion beneath (iii) is expected to be much slower than in (iii) and (iv). Thus

$$G_0'(-\infty) = 0. \tag{5.11c}$$

The solution for G_0 follows from Stewartson & Williams (1973) and gives

$$G_0(-\infty) = -(2\kappa_0)^{\frac{1}{3}} C_0 \quad (C_0 = 1{\cdot}2521\ldots). \tag{5.12}$$

Below the vorticity layer there are two regions (i) and (ii), which in practice may be treated as an entity, the larger and inviscid region (ii), given by

$$0 < Y < A_0/\bar{X}^2,$$

being defined implicitly by the outer limit of the relatively thin sublayer (i), wherein $Y \sim \bar{X}^N$. The index N here is to be found by the need for a viscous interaction to reduce the velocity to zero at the wall $Y = 0$. So, if $\Psi \bar{X}^M$ (M unknown) is a function of $\zeta = Y\bar{X}^{-N}$ in (i), we have $N = M + 1$, from (3.7*a*). Matching (to first order) Ψ as $\zeta \to \infty$ with its value at the lower extremity of (iii), i.e. at $\zeta = A_0/\bar{X}^{N+2}$ from (5.2), we obtain $M + N + 2 = -\frac{2}{3}$. This is because Ψ is approximately linear at the outer edge of (i) owing to the slight adverse pressure gradient [see (5.14) below] promoting the backward motion. Hence $M = -\frac{11}{6}$, $N = -\frac{5}{6}$ and in (i)

$$\Psi \approx \bar{X}^{\frac{11}{6}} g_0(\zeta), \quad \zeta = Y\bar{X}^{\frac{5}{6}}, \tag{5.13}$$

implying that

$$P(X) \approx P_0 - \tfrac{3}{16} P_1 \bar{X}^{\frac{1}{3}} \tag{5.14}$$

and, from the equation of motion,

$$g_0''' - \tfrac{11}{6} g_0 g_0'' + \tfrac{8}{3} g_0'^2 - P_1 = 0. \tag{5.15a}$$

The constraints are $g_0(0) = g_0'(0) = 0$, for no slip, and $g_0'(\infty) = -(\frac{3}{8}P_1)^{\frac{1}{2}}$, the minus sign being necessary to effect the match with (iii). As with (5.3) and (5.4) it was convenient to solve the Falkner–Skan problem for $g_0(\zeta)$ numerically. The solution has the properties

$$g_0''(0) = -1{\cdot}996 \left(\frac{3P_1}{8}\right)^{\frac{3}{4}}, \quad \gamma_0 \equiv \lim_{\zeta \to \infty} \left\{ \left(\frac{8}{3P_1}\right)^{\frac{1}{2}} g_0 + \zeta \right\} = 0{\cdot}4176 \left(\frac{3P_1}{8}\right)^{-\frac{1}{4}}. \tag{5.15b}$$

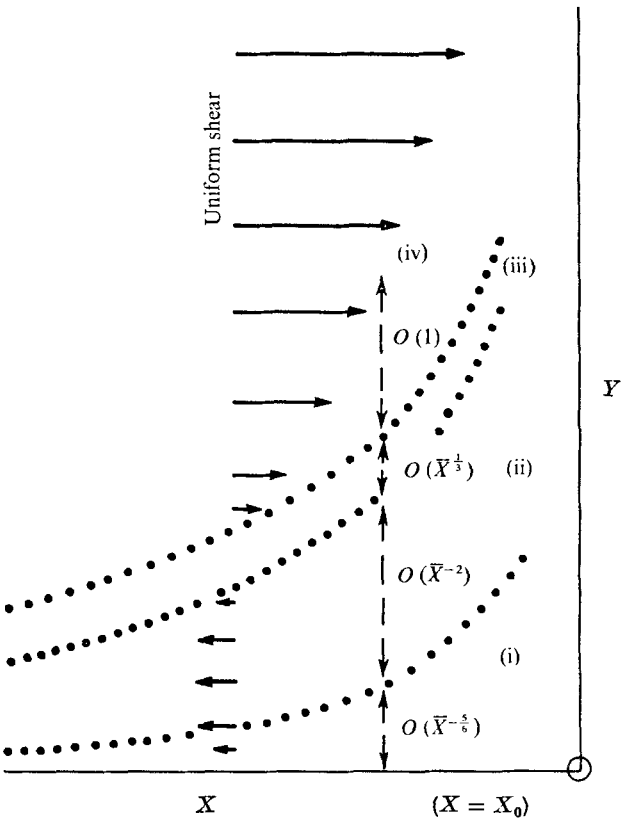

FIGURE 5. The flow structure in layer II near the terminal point; $\bar{X} \ll 1$. Dotted lines indicate the four zones (i)–(iv) and the dashed arrows show their thicknesses. The full arrows represent a velocity profile near $\bar{X} = 0$. (Diagram not to scale.)

The match just mentioned is in essence an equating of the value of Ψ at the lower edge of (iii),

$$\Psi \approx -\bar{X}^{\frac{2}{3}} C_0 (2\kappa_0)^{\frac{1}{3}} + O(\bar{X}) \tag{5.16}$$

from (5.11) and (5.12), with its value outside (ii), where

$$\Psi \approx -(\tfrac{3}{8}P_1)^{\frac{1}{2}} \bar{X}^{\frac{11}{6}} (Y\bar{X}^{\frac{5}{6}} + \gamma_0), \tag{5.17}$$

to assure conservation of mass (cf. Stewartson & Williams 1973). Setting $Y = A_0/\bar{X}^2$ in (5.17), therefore, equating with (5.16) and neglecting the comparatively small terms, we determine P_1 in terms of the known constant C_0 and the unknown factor κ_0:

$$P_1 = \tfrac{50}{3} C_0^2 (2\kappa_0)^{\frac{2}{3}}. \tag{5.18}$$

The whole asymptotic structure of II has now been set down to first order for $\bar{X} \ll 1$ and is shown schematically in figure 5. Above the thin shear layer the flow adjusts to preserve the mass flux constraint, within the shear layer the vorticity is then reduced from the (unknown) constant value just above to zero in its lower reaches, and a small reversed velocity is thereby generated which persists throughout the wider inviscid zone underneath. Finally the reversed

flow is brought to rest in the thin viscous sublayer. The adverse pressure gradient plays little part in this ultimate structure except in the slow-moving sublayer. The matching process near $\bar{X} = 0$ cannot by itself fix even the first-order solution here uniquely, however, and accordingly the profile $\mathscr{F}_0(\bar{Y})$ above the vorticity layer remains undetermined. In practice it is fixed by the solution in $X < X_0$, but no conclusive values for the constants κ_i involved in (5.8) could be drawn from the numerical results. It became increasingly difficult to advance the integrations near the singular point $X = X_0$, whether by use of the Reyhner & Flügge-Lotz scheme or the straightforward technique for $U < 0$, owing presumably to the singular behaviour as $X \to X_0 -$. Further, the comparisons below between the theory and the calculations suggest that $X_0 \approx 0{\cdot}49$ and as our calculations were not marched beyond $X = 0{\cdot}272$ if follows that

$$\{2P_0 - \bar{X}^{\frac{3}{2}} C_0 (2\kappa_0)^{\frac{1}{2}}\}$$

remained negative throughout, whereas ultimately it should become positive. So the profile $\mathscr{F}_0(\bar{Y})$ could take the shear values $\frac{1}{4}\bar{Y}^2$ approximately with an error $(2P_0)$ which did not yield the subsequent contradiction [outlined just below (5.5)] beneath $\bar{Y} = 0$. We may conclude that probably κ_0 is approximately $0{\cdot}25$ but nevertheless the factor $2P_0$, though small numerically, is vital to the terminal profile $\mathscr{F}_0(\bar{Y})$ and introduces the influence of the flow properties in $X < X_0$.

Despite the arbitrariness in II a formal expansion of the solution near $X = X_0$, based on the above analysis, may still be written down for both viscous layers II and III, assuming the form (5.8) for $\mathscr{F}_0(\bar{Y})$ as $\bar{Y} \to 0$, and we outline it here. For $\bar{X} \ll 1$,

$$\left.\begin{aligned} A(X) &= -[A_0/\bar{X}^2 + A_1 \bar{X}^{\frac{3}{2}} - 12P_0 \bar{X}^2 + A_3 \bar{X}^5 + O(\bar{X}^{\frac{11}{2}})], \\ P(X) &= P_0 - \tfrac{3}{16} P_1 \bar{X}^{\frac{16}{3}} - \tfrac{2}{13} P_2 \bar{X}^{\frac{13}{2}} - \ldots, \end{aligned}\right\} \tag{5.19}$$

so that in III, with η as in (5.1),

$$\tilde{\Psi} = \bar{X}^{-\frac{1}{2}} F_0(\eta) + \bar{X}^3 F_1(\eta) + \bar{X}^{\frac{7}{2}} F_2(\eta) + \ldots. \tag{5.20}$$

[The strange powers here and in (5.21)–(5.24) below arise from terms such as β_0 and γ_0 induced in (5.5) and (5.15*b*).] Here F_1, for instance, satisfies the linear equation

$$F_1''' + \tfrac{1}{2} F_0 F_1'' - \tfrac{1}{2} F_0' F_1' - 3F_0'' F_1 = -\tfrac{1}{320} A_1,$$

with $F_1(0) = F_1'(0) = 0$. As $\eta \to \infty$ the outer shear gives

$$F_1 \sim \tfrac{1}{4}(\eta + A_1)^2 - \tfrac{2}{15} A_3,$$

$$F_2 \sim -6P_0 \eta + O(1)$$

on setting $Z = \eta \bar{X}^{\frac{3}{2}}$ and expanding in ascending powers of $\bar{X}$ in the outer condition (3.9*c*). Consistency with the governing equation for F_1 then yields the result $A_1 = \frac{16}{3}\beta_0$. Further inspection reveals that fixing the values of lower-order terms in $A(X)$ requires only the values of the pressure coefficients. In II, when $\bar{Y} \sim 1$

$$\Psi = \mathscr{F}_0(\bar{Y}) + \sum_{n=1}^{5} \bar{X}^n \mathscr{F}_n(\bar{Y}) + \bar{X}^{\frac{16}{3}} \mathscr{F}_6(\bar{Y}) + \ldots, \tag{5.21}$$

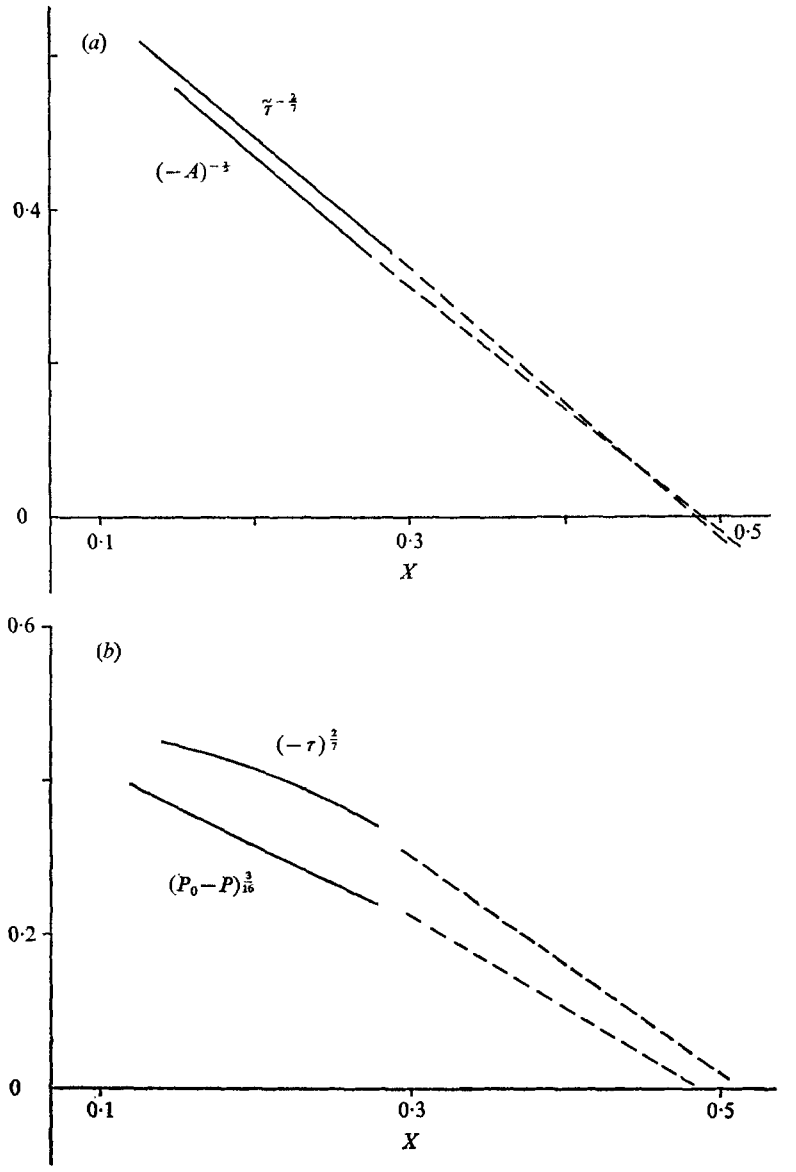

FIGURE 6. (*a*) Variation of $(-A)^{-\frac{1}{2}}$ and $\tilde{\tau}^{-\frac{2}{7}}$ with X. The dashed lines give the corresponding slopes at $X = X_0-$ suggested by (5.1)–(5.5) and (5.27). (*b*) Graphs of $(-\tau)^{\frac{2}{7}}$ and $(P_0-P)^{\frac{3}{16}}$ *vs.* X, with $P_0 = 0{\cdot}11700$. The dashed straight lines are the predictions of (5.13)–(5.15) and (5.27) at $X = X_0-$.

where, from the equations of motion and (5.19), $\mathscr{F}_6(\overline{Y})$, in particular, is given by

$$\mathscr{F}_6(\overline{Y}) = \frac{3P_1}{16}\mathscr{F}_0'(\overline{Y})\int_\infty^{\overline{Y}} \frac{dt}{\mathscr{F}_0'(t)^2}.$$

In the vorticity layer (iii), where $\xi \sim 1$,

$$\Psi = \overline{X}^{\frac{2}{3}}G_0(\xi) + \overline{X}G_1(\xi) + \overline{X}^{\frac{4}{3}}G_2(\xi) + \ldots. \tag{5.22}$$

The function $G_1(\xi)$ is defined by the equation

$$G_1''' - \tfrac{2}{3}G_0 G_1'' + G_0' G_1' - G_1 G_0'' = 0 \tag{5.23}$$

along with the boundary conditions $G_1 \sim (\kappa_1 \xi^3 + 3\kappa_1/\kappa_0 + O(1))$ as $\xi \to \infty$ and $G_1''(-\infty) = 0$. In the sublayer (i), where $\zeta \sim 1$ [see (5.13)],

$$\Psi = \bar{X}^{\frac{11}{8}} g_0(\zeta) + \bar{X}^{\frac{15}{8}} g_1(\zeta) + \ldots, \tag{5.24}$$

with g_1 governed by the differential equation and boundary conditions

$$\left.\begin{aligned} g_1''' - \tfrac{11}{6} g_0 g_1'' + \tfrac{13}{2} g_0' g_1' - 3 g_2'' g_1 &= P_2, \\ g_1(0) = g_1'(0) = 0, \quad g_1'(\infty) &= -\tfrac{2}{13} P_2 (8/3P_1)^{\frac{1}{2}} \end{aligned}\right\} \tag{5.25}$$

to join on to the lower reaches of the vorticity layer (iii). The complete solutions to (5.23) and (5.25) have not been sought but the matching between (i) and (iii) is found to give (cf. Stewartson & Williams 1973) the value

$$P_2 = \tfrac{195}{32} \gamma_0 P_1. \tag{5.26}$$

Hence the entire solution is obtainable in principle and depends solely on the arbitrary profile $\mathscr{F}_0(\bar{Y})$ above the shear layer.

Comparisons of the envisaged structure of the solution as $X \to X_0-$ with the calculated results are on the whole favourable. Figure 5(*a*) shows graphs of $(-A(X))^{-\frac{1}{2}}$ and $(\tilde{\tau}(X))^{-\frac{2}{7}}$ *vs.* X near the termination of the numerical results. According to the analysis both should be linear for $X_0 - X \ll 1$, since (5.1)–(5.5) and (5.13)–(5.15) give

$$\tilde{\tau}(X) \approx 0{\cdot}1488 \bar{X}^{-\frac{7}{2}}, \quad \tau(X) \approx -1{\cdot}996 (\tfrac{3}{8}P_1)^{\frac{3}{4}} \bar{X}^{\frac{7}{2}}. \tag{5.27}$$

The linear forms appear to be verified fairly well and to be not inconsistent with a value

$$X_0 = 0{\cdot}49. \tag{5.28}$$

Similarly, taking $P_0 = 0{\cdot}11700$, a representative value, we plot $(P_0 - P)^{\frac{3}{16}}$, as well as $(-\tau)^{\frac{2}{7}}$, against X in figure 6(*b*). Again the curves may be roughly approximated by a straight line for quite a wide range of $X_0 - X$. In general the theoretical slopes of the straight lines also agree not unfavourably with those implied in (5.1)–(5.18), assuming $\kappa_0 \approx 0{\cdot}25$. Thus it is felt that the predictions of the theory of the singularity are borne out reasonably well.

6. The implications on a finite length scale and discussion

For an imposed asymmetric boundary condition consistent with the scalings of the free-interaction structure set out in § 3, e.g. for an indentation of length $O(aK^{\frac{1}{7}})$ and height $O(aK^{-\frac{3}{7}})$ or an injection rate $\sim ga^2\rho^{-1}\nu^{-1}K^{-\frac{3}{7}}$, the starting profile for the integration of the controlling equations (3.7)–(3.9) past the change in wall properties would need to be chosen from among those in figures 3 and 4. Let us consider an injection or indentation that tends to initiate the interaction studied in § 3, with $b_1 > 0$ in (3.10). Then by analogy with the features of triple-deck studies (Smith & Stewartson 1973; Stewartson 1970), as the severity of the disturbance is increased we can anticipate that a stage is reached where the

necessary starting profile in II has to be a separated one. If the size is thereafter increased indefinitely, the required starting profiles in II and III tend towards those of the ultimate structure detailed in § 5. A corollary of the above description is that, when the asymmetric indentation, say, is of height $O(a)$ then the whole free interaction, from the exponentially small perturbations when X is large and negative to the eventual separated form at $X = X_0-$, must take place before the indentation is reached. Hence the flow adjusts, far upstream, to produce the compressed upper viscous layer III and the partly reversed lower layer II of § 5, which constitute the oncoming flow that is observed at distances only $O(a)$ from the indentation. That a revision of the character of the solution first becomes necessary on this length scale is shown by the behaviour of the core flow I for $X \to X_0-$. There we have

$$u \approx U_\infty(y) - \epsilon^2 A_0 U'_\infty(y)/\bar{X}^2 \tag{6.1}$$

from (3.3), (3.4) and (5.2), and so the core flow is no longer a small perturbation of the Poiseuille flow when $\bar{X} \sim \epsilon$, i.e. when x is $O(a)$. In fact it is gratifying to find that, upon conversion to a length scale comparable with the width of the channel, the rather strange-looking powers and factors involved in the structure of the singularity take on a seemingly sensible physical character. In particular, if $-x^*$ now denotes distances upstream of this $O(a)$ indentation, and correspondingly $a\bar{X} = a(X_0 - X)$ measures distances upstream on the free-interaction scale, then, since $\bar{X} = -\epsilon x^*/a$, the thickness of the compressed slip layer in III becomes $a\epsilon^2(-\epsilon x^*/a)^{\frac{3}{2}}$, from (2.8) and (5.1), i.e.

$$K^{-\frac{1}{2}} a^{-\frac{1}{2}} (-x^*)^{\frac{3}{2}} \tag{6.2}$$

in physical terms. Similarly the thickness of the shear layer (iii) in the lower viscous region as $X \to X_0-$ is $O(a\epsilon^2(-\epsilon x^*/a)^{\frac{1}{3}})$, or $O(a^{\frac{2}{3}} K^{-\frac{1}{3}} / x^{*\frac{1}{3}})$ physically as $x^* \to -\infty$, while the relative errors $\bar{X}^{\frac{7}{2}}$ and $\bar{X}^{\frac{7}{6}}$ in (5.19) and (5.24) indicate corrections of orders $K^{-\frac{1}{2}}$ and $K^{-\frac{1}{6}}$ when $x^* \sim a$. Converting the other facets of the singularity into physical terms we obtain the following description of the oncoming flow for $x^* \to -\infty$ but $|x^*| \ll aK^{\frac{1}{7}}$:

$$\text{pressure } p^* \approx \begin{cases} \text{constant} - \frac{3}{16} P_1 K^{-\frac{1}{3}} (-x^*/a)^{\frac{16}{3}} ag & \text{(near lower wall)}, \quad (6.3a) \\ -\frac{1}{50} K (-x^*/a)^{-4} ag & \text{(near upper wall)}, \quad (6.3b) \end{cases}$$

$$\text{velocity } u^* \approx ga^2/\rho\nu \begin{cases} U_\infty(y^*/a) - 2/5x^{*2} U'_\infty(y^*/a) & \text{(in core)}, \quad (6.3c) \\ (-x^*/a)^{-2} F'_0(\eta) & \text{(in III)}, \quad (6.3d) \\ K^{-\frac{1}{3}} (-x^*/a)^{\frac{1}{3}} G'_0(\xi) & \text{(in shear layer)}, \quad (6.3e) \\ K^{-\frac{2}{3}} (-x^*/a)^{\frac{5}{3}} g'_0(\zeta) & \text{(in reversed flow)}, \quad (6.3f) \end{cases}$$

$$\text{width of reversed flow region} \approx \begin{cases} \frac{2}{5} a (a/x^*)^2 & \text{(inviscid part)}, \quad (6.3g) \\ K^{-\frac{1}{6}} a (-x^*/a)^{-\frac{5}{6}} & \text{(viscous sublayer)}. \quad (6.3h) \end{cases}$$

A brief formal account of the properties of the fluid motion locally, within distances $O(a)$ of the indentation, may therefore be written down from (6.1)–(6.3). For $0 < S(x) < y < 1$ a forward-moving core flow exists in which u and v are $O(1)$ and p is $O(K)$ when $x \sim 1$. Here $y = S(x)$ defines the position of the detached

viscous shear layer. Hence the motion in the core is now governed by the non-linear inviscid equations

$$\left.\begin{aligned} &\partial u/\partial x+\partial v/\partial y=0,\\ &u\frac{\partial u}{\partial x}+v\frac{\partial u}{\partial y}=-\frac{\partial p}{\partial x},\\ &u\frac{\partial v}{\partial x}+v\frac{\partial v}{\partial y}=-\frac{\partial p}{\partial y} \end{aligned}\right\} \tag{6.4}$$

together with the boundary conditions $v=0$ at $y=1$ (tangential flow), $u=v=0$ at $y=S(x)$ (no slip at the shear layer) and

$$\left.\begin{aligned} u &\sim U_\infty(y)-(2/5x^2)\,U'_\infty(y)+\dots\\ v &\sim(-4/5x^3)\,U_\infty(y)+\dots\\ p &\sim-\frac{12}{5x^3}\int_0^y U_\infty^2(t)\,dt+\dots \end{aligned}\right\} \quad \text{for } x\to-\infty. \tag{6.5}$$

(In terms of the stream function ψ, (6.4) gives the vorticity equation $\nabla^2\psi=f(\psi)$, where f is an unknown function of ψ.) Near the upper wall a slip layer of thickness $O(aK^{-\frac{1}{2}})$ is induced, to reduce the velocity to zero at the wall; in this layer the boundary-layer equations apply:

$$\frac{\partial u}{\partial x}+\frac{\partial\tilde v}{\partial\tilde y}=0,\quad u\frac{\partial u}{\partial x}+\tilde v\frac{\partial u}{\partial\tilde y}=-\frac{dp}{dx}+\frac{\partial^2 u}{\partial\tilde y^2}. \tag{6.6}$$

Here $\tilde y=(1-y)\,K^{\frac{1}{2}}$ and $\tilde v=-vK^{\frac{1}{2}}$ are $O(1)$, $u\to\tilde U_1(x)$ as $\tilde y\to\infty$ and $u=\tilde v=0$ at $\tilde y=0$, where $\tilde U_1(x)$ is the slip velocity of the core at the upper wall. For x large and negative the solution is given by

$$\left.\begin{aligned} u &= x^{-2}F'_0(\eta)+\dots,\\ \tilde v &= -\tfrac{1}{2}x^{-\frac{3}{2}}[F_0(\eta)+3\eta F'_0(\eta)]+\dots, \end{aligned}\right\} \tag{6.7}$$

with $\tilde U_1(x)\approx 1/5x^2$, where $\eta=\tilde y(-x)^{-\frac{3}{2}}$ from (5.1). Around the free streamline $y=S(x)$, whose shape has to be determined, a viscous layer of thickness $O(aK^{-\frac{1}{3}})$ reduces the vorticity from the core value at its upper edge to zero below. Again the boundary-layer equations apply, but without a pressure gradient, and $u\to\kappa(x)\,\bar y+o(1)$ as $\bar y=(y-S(x))\,K^{\frac{1}{3}}\to\infty$, where $\kappa(x)$ is the shear stress of the core at $y=S(x)$, and $u\to 0$ as $\bar y\to-\infty$. Beneath the shear layer there is a slow, inviscid, reversed flow for $0<y<S(x)$. Between that and the lower wall the thin viscous sublayer, where $\hat y=yK^{\frac{1}{3}}\sim 1$, is invoked to bring the reversed velocity to zero at $\hat y=0$. In this sublayer $u\sim K^{-\frac{2}{3}}$, $v\sim K^{-\frac{1}{3}}$ and the adverse pressure gradient $p'(x)\sim K^{-\frac{1}{3}}$, so that the relevant boundary-layer equations hold with $u=v=0$ at $\hat y=0$ and $u\to\hat U(x)$ (<0 upstream) as $\hat y\to\infty$, where $\frac{1}{2}\hat U^2+p(x)=$ constant. Determination of $p(x)$ then requires matching the stream function in the slip layer with that at the lower edge of the vorticity layer, in the manner of § 5. That the structure of layer II near the singularity $X=X_0-$, as revealed in § 5, does also provide the asymptotic solution to the shear-layer and sublayer flows for $x\to-\infty$ may be verified.

In summary, then, the suggestion is that the local flow at finite distances from the obstruction does not involve a direct continuation from the Poiseuille flow. Rather, the Poiseuille flow must first be altered, at a great distance $[O(aK^{\frac{1}{7}})]$ upstream, via the whole free interaction; the local flow then joins on

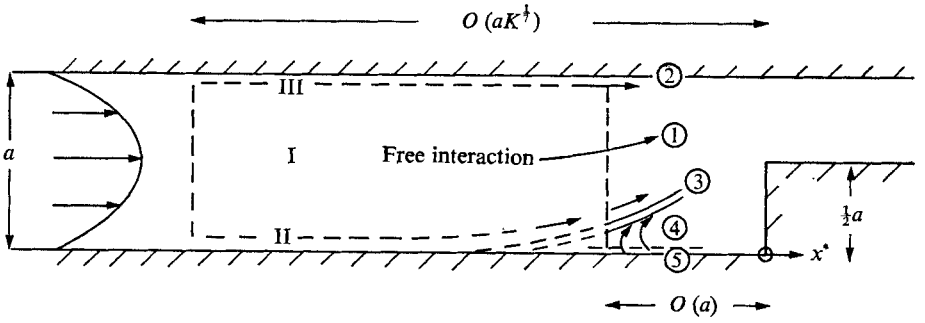

FIGURE 7. Schematic diagram (not to scale) of the upstream flow pattern envisaged for a channel whose width is abruptly halved. The long, free, interaction converts the oncoming Poiseuille flow into a five-tiered structure (①–⑤) for $|x^*| \sim a$: ①, core; ②, slip layer; ③, detached shear layer; ④, slow inviscid backward-moving region; ⑤, slow viscous backward-moving region.

to the terminal form of this interaction, in the manner of (6.5) and (6.7). In particular, separation occurs at a position $0{\cdot}49aK^{\frac{1}{7}}$ upstream [from (5.28)], after which it is perfectly sensible, physically, that the terminal form should involve a singularity of the type discussed in § 5. For that means that the typical length scale undergoes the required shortening, straight from $O(aK^{\frac{1}{7}})$ to $O(a)$ [according to (6.1)], as the indentation itself is approached. Although, on the long scale (X finite), the asymmetric indentation is actually sited right at the terminal point $X = X_0$, it is at a distance $O(a)$ from that singular region. The main indeterminacy in the upstream adjustment is then the *precise* positioning of the indentation relative to the point $X = X_0$, e.g. in (6.5) and (6.7) we could replace x by $x+d$, where d is a finite constant, and still achieve the match with the free-interaction solution. In fact, the influence of the specific conditions downstream is first felt only through the displacement factor d. Another point worth noting is that the upstream decay of the flow perturbations is algebraic when observed from a finite station ($x \to -\infty$, but $|X - X_0| \ll 1$), but is exponential when observed on the long scale ($X \to -\infty$). Figure 7 illustrates the proposed structure of the high Reynolds number flow on nearing the indentation.

Comparisons of this theory with the numerical solutions of the full Navier–Stokes equations by Hurd & Peters (1970), for a sharp 90° bend in the channel, and by Greenspan (1969) and Friedman (1972), for a finite or semi-infinite step, are not unfavourable. On the qualitative side, both of these asymmetric distortions do produce a sizable upstream adjustment of the flow when the Reynolds number is large, as we should predict. For instance, with the step (Greenspan 1969), the flow separates at one wall (for values of K greater than about 2000) and, as the Reynolds number increases, the size of the reversed flow zone grows and the shear stress at the other wall achieves increasingly high values upstream. Also, the dividing streamline ($y = S(x)$) upstream in Greenspan, figures 4 and 5, certainly exhibits the concave-upwards behaviour (for all values of K) that is implied by the result in (6.3), i.e. $S(x) \sim 2/5x^2$ for x large and negative (when $K \gg 1$). With the 90° bend (Hurd & Peters 1970), the pressure falls sharply at the 'inside' of the bend and the shear stress at the 'outside' falls, in line with

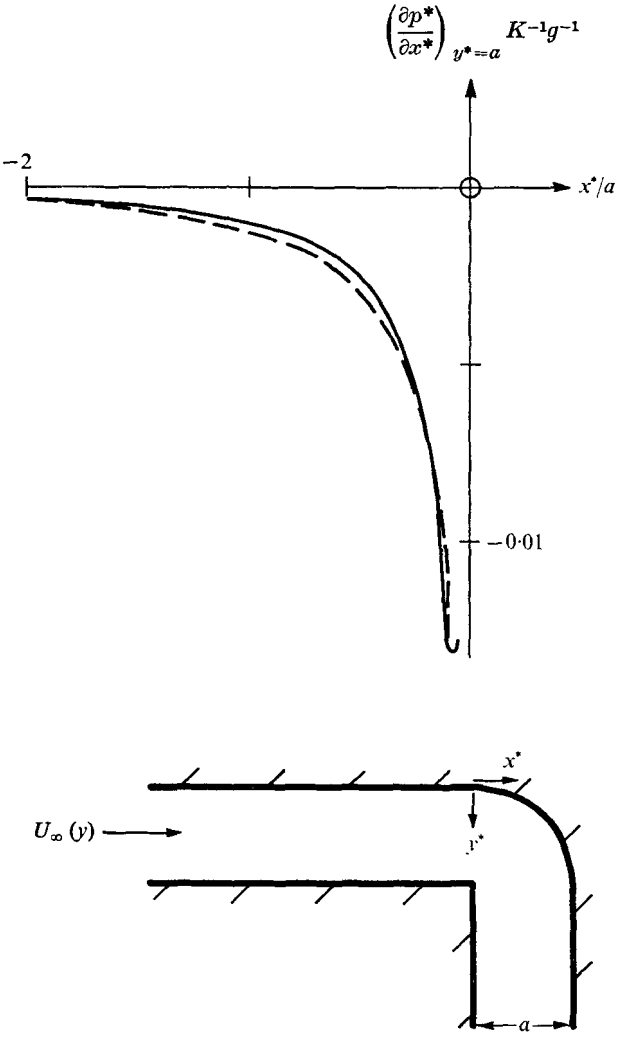

FIGURE 8. The pressure gradient at the inner wall ($y^* = a$) ahead of a 90° bend. ——, from Hurd & Peters (1970) figure 7, at $K = 6400$; – – –, asymptotic result (6.8).

§§ 5 and 6 above (although Hurd & Peters' figure 3 exhibits no flow reversal at $K = 6400$). A third example of a finite disturbance is provided by Matida, Kuwahara & Takami's (1975) numerical study of flow past an interior blockage. They calculated solutions only for moderate Reynolds numbers, but there is evidence (see their figure 5) of a pronounced reduction upstream in the shear stress at one wall, and of a corresponding increase at the other wall, which does support the present asymptotic description to some extent. Reasonable agreement is also indicated by two quantitative comparisons, the first being with Hurd & Peters' results for the pressure gradient $\partial p^*/\partial x^*$ at the inner wall. Our proposal is, for x^* large and negative (but $|x^*| \ll aK^{\frac{1}{7}}$),

$$(\partial p^*/\partial x^*)_{y^*=a} \approx 2Kg/25(x+d)^5 \tag{6.8}$$

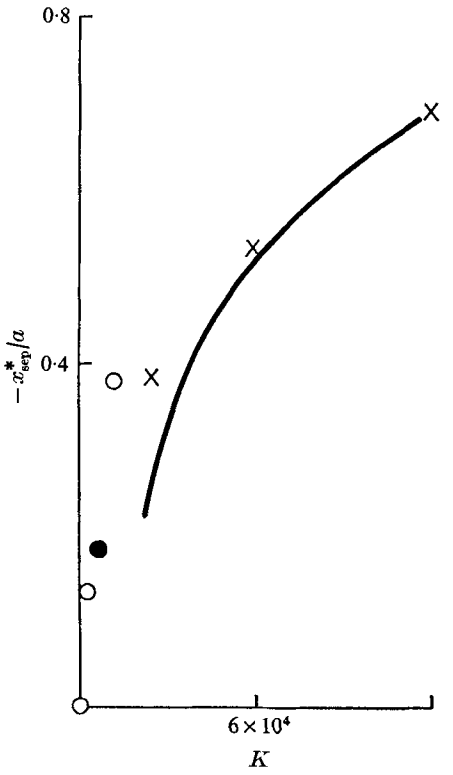

FIGURE 9. The dependence of the upstream separation point on the Reynolds number K. The theoretical prediction of (6.9) (solid curve) is compared with the numerical results of Greenspan for a semi-infinite step (crosses) and with the numerical results of Greenspan (open circles) and Friedman (filled circle) for a finite step.

from (6.5), and is plotted with Hurd & Peters' upstream results in figure 8. The constant d, corresponding to an origin shift, is not given by the asymptotic theory as yet, but in figure 8 we choose the value $d = -1{\cdot}4$ to ensure close agreement at $x = -2$. The asymptotic curve then follows the full solutions fairly closely up to about $x = -0{\cdot}2$, at which stage the bending itself, starting at $x = 0$, exerts a dominant influence. Second, the separation point $x^* = x^*_{\rm sep}$, which is predicted as

$$x^*_{\rm sep} = -0{\cdot}49aK^{\frac{1}{7}} + O(a) \tag{6.9}$$

asymptotically, is compared in figure 9 with that found in Greenspan's calculations for a semi-infinite step and for a finite step (Friedman's later calculations appear to confirm Greenspan's results on the whole). Again a suitable choice, $1{\cdot}96a$, for the finite constant '$O(a)$' in (6.9) is made, to bring (6.9) into line with Greenspan's value at $K = 12\times10^4$. The trend of the purely numerical results is then not inconsistent with (6.9) as the Reynolds number increases. A different choice for the $O(a)$ term in (6.9) would improve the agreement for the finite-step results. Overall, in view of the fact that $\epsilon = K^{-\frac{1}{7}}$ takes values greater than $0{\cdot}18$ in the full numerical solutions above (e.g. in figure 8, $\epsilon = 0{\cdot}286$; also, the separation points in figure 9 still occur not far upstream even at $K = 12\times10^4$), whereas

the present asymptotic theory certainly requires $\epsilon \ll 1$, the measure of agreement is thought to be encouraging.

The determination of the entire motion through the asymmetrically distorted channel, for $-\infty < x < \infty$, when the Reynolds number is large remains a formidable task, of course. We believe, however, that a self-consistent account of the flow adjustment that takes place far ahead of any finite change in the wall or interior conditions has been put forward in this paper, and that it is of practical value.

I am grateful to the referees for their helpful suggestions on the presentation, and in particular to the referee who pointed out most of the full numerical solutions referred to above.

REFERENCES

FRIEDMAN, M. 1972 Laminar flow in a channel with a step. *J. Engng Math.* **6**, 285.

GOLDSTEIN, S. 1948 On laminar boundary layer flow near a point of separation. *Quart. J. Mech. Appl. Math.* **1**, 43.

GREENSPAN, D. 1969 Numerical studies of steady, viscous, incompressible flow in a channel with a step. *J. Engng Math.* **3**, 21.

HURD, A. C. & PETERS, A. R. 1970 Analysis of flow separation in a confined two-dimensional channel. *Trans. A.S.M.E., J. Basic Engng*, **92**, 908.

KELLER, H. B. & CEBECI, T. 1971 Accurate numerical methods for boundary layer flows. I. Two-dimensional laminar flows. *2nd Int. Conf. Num. Meth. in Fluid Dyn.*, p. 92. Springer.

MATIDA, Y., KUWAHARA, K. & TAKAMI, H. 1975 Numerical study of steady two-dimensional flow past a square cylinder in a channel. *J. Phys. Soc. Japan*, **38**, 1522.

MESSITER, A. F. 1970 Boundary layer flow near the trailing edge of a flat plate. *S.I.A.M. J. Appl. Math.* **18**, 241.

REYHNER, T. A. & FLÜGGE-LOTZ, I. 1968 The interaction of a shock wave with a laminar boundary layer. *Int. J. Nonlinear Mech.* **3**, 173.

SMITH, F. T. 1973 Laminar flow over a small hump on a flat plate. *J. Fluid Mech.* **57**, 803.

SMITH, F. T. 1974 Boundary layer flow near a discontinuity in wall conditions. *J. Inst. Math. Appl.* **13**, 127.

SMITH, F. T. 1976*a* Flow through constricted or dilated pipes and channels. *Quart. J. Mech. Appl. Math.* **29**, 343.

SMITH, F. T. 1976*b* Flow through constricted or dilated pipes and channels. Part 2. *Quart. J. Mech. Appl. Math.* **29**, 365.

SMITH, F. T. 1976*c* On entry-flow effects in bifurcating, blocked or constricted tubes. *J. Fluid Mech.* **78**, 709.

SMITH, F. T. & STEWARTSON, K. 1973 On slot-injection into a supersonic laminar boundary layer. *Proc. Roy. Soc.* A **332**, 1.

STEWARTSON, K. 1969 On the flow near the trailing edge of a flat plate II. *Mathematika*, **16**, 106.

STEWARTSON, K. 1970 On supersonic laminar boundary layers near convex corners. *Proc. Roy. Soc.* A **319**, 289.

STEWARTSON, K. 1974 Multistructured boundary layers on flat plates and related bodies. *Adv. in Appl. Mech.* **14**, 145.

STEWARTSON, K. & WILLIAMS, P. G. 1969 Self-induced separation. *Proc. Roy. Soc.* A **312**, 181.

STEWARTSON, K. & WILLIAMS, P. G. 1973 Self-induced separation II. *Mathematika*, **20**, 98.

WILSON, S. D. R. 1969 The development of Poiseuille flow. *J. Fluid Mech.* **38**, 793.